**Smart Structures and Systems**, *Vol. 26, No. 2 (2020) 185-193*
DOI: https://doi.org/10.12989/sss.2020.26.2.185


# Nonlinear forced vibration of sandwich plate with considering FG core and CNTs reinforced nano-composite face sheets

Rasoul Rostami [b], Mohsen Irani Rahaghi* and Mehdi Mohammadimehr [a]

*Department of Solid Mechanics, Faculty of Mechanical Engineering, University of Kashan, Kashan 87317-53153, Iran*

(*Received April 13, 2019, Revised May 29, 2020, Accepted July 21, 2020*)

**Abstract.** Nonlinear vibration of sandwich plate with functionally graded material (FGM) core and carbon nano tubes reinforced (CNTs) nano-composite layers by considering temperature-dependent material properties are studied in this paper. Base on Classical plate theory (CPT), the governing partial differential equations of motion for sandwich plate are derived using Hamilton principle. The Galerkin procedure and multiple scales perturbation method are used to find relation between nonlinear frequency and amplitude of vibration response. The dynamic responses of the sandwich plate are also investigated in both time and frequency domains. Then, the effects of nonlinearity, excitation, power law index of FG core, volume fraction of carbon nanotube, the function of material variations of FG core, temperature changes, scale transformation parameter and damping factor on the frequency responses are investigated.

**Keywords:** nonlinear vibration; sandwich plate; FG core and FG-CNTs face sheets; nano-composite; multiple scales perturbation method

## 1. Introduction

As a common structure that has many applications in aerospace, automobile and mechanical engineering is the sandwich plate. So that investigating its static and dynamic responses and stability of this structure has big aspect and many research done in this field.

Chien and chen (2005) studied the nonlinear vibrations of laminated plate on a nonlinear elastic foundation, they used the Galerkin's approximate procedure and Runge–Kutta method for reduce the governing nonlinear partial differential equations into the ordinary nonlinear differential equations and finding the ratio of nonlinear frequency to the linear frequency. Chein and Chen (2006) investigated the effect of initial stresses on the nonlinear vibrations of laminated plates placed on the elastic foundation. Singha and Daripa (2009) used the shear deformable finite element method to analyze the large amplitude flexural vibration characteristics of composite plates under transverse harmonic pressure or periodic in-plane load. They showed the steady-state or unsteady nature of the flexural vibration under different loading and boundary conditions by drawing the time history diagram. Xue *et al*. (2011) based on the von Karman plate theory for large deflection, analyzed the non-linear principal resonance of an orthotropic magnetoelastic rectangular plate. They employed the Bubnov– Galerkin method to change the non-linear partial differential equation into a third-order nonlinear ordinary differential equation, and then by using multiple-scale method, found the equation between the amplitude and frequency of system. Their results showed the effects of the magnetic field, orthotropic material property, plate thickness, and the mechanical load on the principal resonance behavior. Liu and Chu (2012) presented the nonlinear vibrations of rotating circular cylindrical shell by using Hamilton principle and Galerkin's method. The effects of nonlinearity, excitation and damping on frequency responses of steady state solution are investigated. Alijani and Amabili (2013) considered the nonlinear vibrations of completely free laminated and sandwich rectangular plates. For driving the equations of motion, they used the multi-modal energy approach based on Lagrange equations and by using classical and higher-order shear deformation theories and Von Karman type nonlinearities. Their results presented the frequency-response curves, time histories and phase space diagrams. Based on nonlinear Von Karaman's theory for thin plates and hierarchical finite element method, Houmat (2013) analyzed the nonlinear free vibration of laminated composite rectangular plates with curvilinear fibers. The fiber orientation angles and layup sequence were shown to affect the degree of hardening and mode shapes. Kattimani and Ray (2014) studied the active constrained layer damping (ACLD) of large amplitude vibrations of smart magneto-electro-elastic (MEE) plates. Razavi and Shooshtari (2014) investigated the nonlinear free vibration of symmetric magneto-electro-elastic laminated rectangular plates with simply supported boundary conditions. Maxwell equations for electrostatics and magnetostatics used to model the electric and magnetic behaviors. Perturbation method was used to solve the equations of motion, analytically and a closed-form relation

*Corresponding author, Ph.D.,
E-mail: Irani@kashanu.ac.ir
[a] Ph.D., E-mail: mmohammadimehr@kashanu.ac.ir
[b] Ph.D. Student, E-mail: R_rostami@grad.kashanu.ac.ir


http://www.techno-press.org/?journal=sss&subpage=7
ISSN: 1738-1584 (Print), 1738-1991 (Online)

was obtained for the nonlinear frequency ratio. Shen and Xiang (2014) presented the large amplitude vibration behavior of nanocomposite cylindrical panels resting on elastic foundations in thermal environments. Numerical results demonstrated that the natural frequencies of the CNTRC panels were reduced but the nonlinear to linear frequency ratio of the CNTRC panels was increased as the temperature rise. Solanki *et al*. (2015) by using meshless technique based on multi quadric radial basis function (MQRBF) examined the nonlinear free vibration response of shear deformable laminated composite and sandwich plates. Their results demonstrated the effects of aspect ratio, span to thickness ratio, orthotropy ratio of the material and fiber orientation on the frequency. Chaudhari et al. (2016) presented the nonlinear vibration response of shear deformable functionally graded plate using finite element method. They investigated the effect of nonlinear kinematics, thickness ratio, amplitude ratio and the volume fraction ratio on the vibration characteristics of FGM plate. Duc *et al*. (2016) derived the governing equations of motion for nonlinear dynamic response and vibrations of a plate made of piezoelectric functionally graded materials that was reinforced by eccentrically outside stiffeners with piezoelectric actuators resting on Pasternak type elastic foundations subjected to mechanical and electrical loads in thermal environments. They discussed the effects of geometrical parameters; material properties; imperfections; elastic foundations; stiffeners and thermal stress in stiffeners; mechanical and electrical loads, temperature on the nonlinear dynamic response and vibration of the piezoelectric FGM plates. Torabi and Ansari (2017) studied the nonlinear free vibration analysis of thermally induced FG-CNTRC annular plates. Darabi and Ganesan (2017) analyzed the dynamic instability of thin laminated composite plates subjected to harmonic in-plane loads. They solved the nonlinear large deflection plate equations of motion by using Galerkin's technique that leads to a system of nonlinear Mathieu-Hill equations. Their results indicated the effects of the orthotropy, magnitude of both tensile and compressive longitudinal loads, aspect ratios of the plate including length-to-width and length-to-thickness ratios, and in-plane transverse wave number on the parametric resonance particularly the steady-state vibrations amplitude. Soni *et al*. (2017) based on classic plate theory (CPT) presented the nonlinear analytical model for the transverse vibration of cracked magneto-electro-elastic (MEE) thin plate. Golami and Ansari (2018) examined the geometrically nonlinear harmonically excited vibration of third-order shear deformable functionally graded graphene platelet-reinforced composite (FG-GPLRC) rectangular plates with different edge conditions. Their results plotted in the form of frequency-response and force-response curves to show the effects of different parameters such as GPL distribution pattern, weight fraction, geometry of GPL nanofillers and boundary constraints of FG-GPLRC plates. Nematollahi and Mohammadi (2019) based on higher-order nonlocal strain gradient theory analyzed the nonlinear vibration of symmetric and also antisymmetric sandwich nanoplates. Their results indicated the effects of small-scale parameter on nonlinear behavior of sandwich nanoplate. Zeng *et al*. (2019) investigated the nonlinear vibration of piezoelectric sandwich nanoplates with functionally graded porous core under electrical loads. Teng and Wang (2020) studied the nonlinear free vibration of rectangular plates reinforced with 3D graphene foam. Their results showed that the nonlinear frequencies of 3D-GFR plates increased as the skeleton weight fraction increased. The effect of negative Poisson's ratio on linear and nonlinear of temperature-dependent FG-CNTRC laminated plates investigated by Yang *et al*. (2020).

In this paper, the nonlinear vibration of sandwich plate will be analyzed based on Classical plate theory (CPT). The structure is formed with FGM core and carbon nano tubes reinforced (CNTs) nano-composite layers by considering temperature-dependent material properties. The governing equations and the corresponding boundary conditions are established through the Hamilton principle. The multiple scales perturbation method will be used for finding the relation between amplitude and nonlinear frequency of the system, and then the effects of various parameters are investigated such as different types of FG material variation function, power law index of FG core, volume fraction of carbon nanotube, temperature changes, scale transformation parameter and linear damping factor on amplitude - frequency diagram.

## 2. Governing equations of motion

The sandwich plate is considered, as shown in Fig. 1 where $a$ is the length of the plate, $b$ is the width, $h$ is the thickness of core, and $h_p$ is the thickness of top and bottom layers. A Cartesian coordinate system ($x$, $y$, $z$) is considered that the z direction denotes thickness of the sandwich plate.

### *2.1 Obtaining the equilibrium equations of sandwich*

Classic plate theory (CPT) used to model the behaviour of sandwich plate (Shahverdi and Khalafi 2016), the $u$, $v$ and $w$ denote the displacements of any point of the sandwich plate with respect to $x$, $y$ and $z$ directions, respectively.

$$U(x,y,z) = u(x,y) - z\frac{\partial w}{\partial x} \tag{1}$$

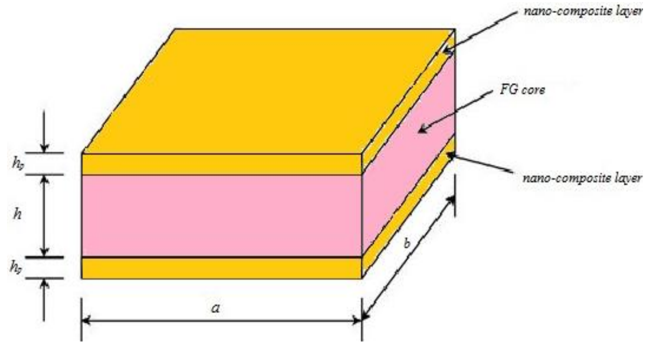


Fig. 1 Schematic of a sandwich plate with considering FG core and CNTs reinforced nano-composite face sheets

$$V(x,y,z)=v(x,y)-z\frac{\partial w}{\partial y} \tag{2}$$

$$W(x,y,z)=w(x,y) \tag{3}$$

By considering the large deformation, the strain field of the sandwich plate becomes

$$\varepsilon=\varepsilon^0+z\Upsilon \tag{4}$$

Where

$$\varepsilon=\begin{Bmatrix}\varepsilon_x\\ \varepsilon_y\\ \gamma_{xy}\end{Bmatrix},\qquad \varepsilon^0=\begin{Bmatrix}\frac{\partial u}{\partial x}+0.5(\frac{\partial w}{\partial x})^2\\ \frac{\partial v}{\partial y}+0.5(\frac{\partial w}{\partial y})^2\\ \frac{\partial v}{\partial x}+\frac{\partial u}{\partial y}+\frac{\partial w}{\partial x}\frac{\partial w}{\partial y}\end{Bmatrix},$$
$$\Upsilon=\begin{Bmatrix}-\frac{\partial^2 w}{\partial x^2}\\ -\frac{\partial^2 w}{\partial y^2}\\ -2\frac{\partial^2 w}{\partial x\partial y}\end{Bmatrix} \tag{5}$$

The thermo-elastic stress–strain relation of sandwich plate in FG core is given by (Mohammadimehr *et al.* 2016a)

$$\begin{Bmatrix}\sigma_x\\ \sigma_y\\ \tau_{xy}\end{Bmatrix}=\begin{bmatrix}Q_{11}^C & Q_{12}^C & 0\\ Q_{12}^C & Q_{22}^C & 0\\ 0 & 0 & Q_{44}^C\end{bmatrix}\begin{Bmatrix}\varepsilon_x\\ \varepsilon_y\\ \gamma_{xy}\end{Bmatrix}-\begin{Bmatrix}\alpha_x^C\\ \alpha_y^C\\ 0\end{Bmatrix}\Delta T \tag{6}$$

$Q_{ij}^C$ are the stiffness components of the FG core that are defined as follow

$$Q_{11}^C=\frac{E(z)}{1-\nu(z)^2},\quad Q_{12}^C=\frac{\nu E(z)}{1-\nu(z)^2},\quad Q_{44}^C=\frac{E(z)}{2(1+\nu(z))}$$

$E(z)$ and $\nu(z)$ are Young's modulus and Poisson's ratio, respectively.

The general models that have been presented in literature for these variation properties (here it is denoted by a general variable p) can be categorized into three types: power-law functions (P-FGM), sigmoid functions (S-FGM) and exponential functions (E-FGM) with the following relations (Asnafi and Abedi 2015), respectively.

$$p(z)=(p_1-p_2)(\frac{z}{h}+0.5)^n+p_2\text{(P-FGM)} \tag{7a}$$

$$p(z)=\begin{cases}0.5(1+\frac{2z}{h})^n(p_1-p_2)+p_2 for -\frac{h}{2}\le z\le 0\\ [1-0.5(1-\frac{2z}{h})^n](p_1-p_2)+p_2 for 0\le z\le\frac{h}{2}\end{cases} \tag{7b}$$
(S-FGM)

$$p(z)=p_2\,exp\left[\left(\frac{z}{h}+0.5\right)ln\left(\frac{p_1}{p_2}\right)\right]\text{(E-FGM)} \tag{7c}$$

In relation (7), $n$ is the material parameter, where $p_1$ and $p_2$ are the material properties of the lower ($z$ = $h$/2) and upper ($z$ = -$h$/2) surface of the plate, respectively.

The thermo-elastic stress–strain relation of sandwich plate in nanocomposite layer is given by (Mohammadimehr *et al.* 2016b)

$$\begin{Bmatrix}\sigma_x\\ \sigma_y\\ \tau_{xy}\end{Bmatrix}=\begin{bmatrix}Q_{11}^f & Q_{12}^f & 0\\ Q_{12}^f & Q_{22}^f & 0\\ 0 & 0 & Q_{44}^f\end{bmatrix}\begin{Bmatrix}\varepsilon_x\\ \varepsilon_y\\ \gamma_{xy}\end{Bmatrix}-\begin{Bmatrix}\alpha_x^f\\ \alpha_y^f\\ 0\end{Bmatrix}\Delta T \tag{8}$$

$Q_{ij}^f$ are the stiffness components of the nanocomposite layers that defined as follow

$$Q_{11}^f=\frac{E_{11}}{1-\upsilon_{12}^2},\qquad Q_{22}^f=\frac{E_{22}}{1-\upsilon_{12}^2},$$
$$Q_{12}^f=\frac{\nu_{12}E_{11}}{1-\nu_{12}^2},\qquad Q_{44}^f=G_{23} \tag{9}$$

$E_{11}$, $E_{22}$, $G_{12}$ and $\upsilon_{12}$ are Young's modulus, shear modulus and Poisson's ratio, respectively.

In the extended rule of mixture (ERM) approach, material properties of the nanocomposite face sheet of sandwich plates reinforced by single-walled nanotube (SWNT) are considered as (Mohammadimehr *et al.* 2016b)

$$E_{11}=\eta_1 V_{CNT}E_{11}^{CNT}+V_mE^m \tag{10}$$

$$\frac{\eta_2}{E_{22}}=\frac{V_{CNT}}{E_{22}^{CNT}}+\frac{V_m}{E^m} \tag{11}$$

$$\frac{\eta_3}{G_{12}}=\frac{V_{CNT}}{G_{12}^{CNT}}+\frac{V_m}{G^m} \tag{12}$$

$$\nu_{12}=V_{CNT}\nu_{12}^{CNT}+V_m\nu^m \tag{13}$$

$$\rho=V_{CNT}\rho^{CNT}+V_m\rho^m \tag{14}$$

$$\alpha_x^f=\frac{V_{CNT}E_{11}^{CNT}\alpha_x^{CNT}}{V_{CNT}E_{11}^{CNT}+V_mE^m} \tag{15}$$

$$\alpha_y^f=(1+\nu_{12}^C)V_{CNT}\alpha_y^{CNT}+(1+\nu^m)V_m\alpha^m-\nu_{12}\alpha_x^f \tag{16}$$

where $E_{11}^{CNT}$, $E_{22}^{CNT}$, $G_{12}^{CNT}$, $E^m$, $G^m$, $\alpha_x^{CNT}$ and $\alpha_\theta^{CNT}$ are Young's modulus, shear modulus of carbon nanotube and the matrix and thermal expansion coefficients, respectively. $V_{CNT}$ and $V_m$ are volume fraction of carbon nano-tube and the matrix, respectively.

$$V_m+V_{CNT}=1 \tag{17}$$

The elastic strain energy of the sandwich plate with thickness ($h$ + 2$h_p$) is expressed with the classical assumption of plane stress

$$U=\int_v(\sigma_x\varepsilon_x+\sigma_y\varepsilon_y+\tau_{xy}\gamma_{xy})dV \tag{18}$$

The transverse excitation subjected to the sandwich plate is expressed as follow

$$F(t) = F_0 \cos(\omega t) \tag{19}$$

Where $F_0$ is the amplitude of excitation and ω represents frequency of the excitation.

Consequently, the virtual work performed by external force is expressed as

$$\delta W = \iint_A F \delta W dA = \int_0^a \int_0^b F \delta W dy dx \tag{20}$$

In the following analysis, substituting (18) and (20) into the Hamilton equation, the governing equations of the sandwich plate are derived as follow

$$\delta u: N_{x,x} + N_{xy,y} = 0 \tag{21}$$

$$\delta v: N_{y,y} + N_{xy,x} = 0 \tag{22}$$

$$\begin{aligned} \delta w: \quad & N_{x,x} w_{0,x} + N_x w_{0,xx} - M_{x,xx} + N_{y,y} w_{0,y} \\ & + N_y w_{0,yy} - M_{y,yy} + N_{xy,x} w_{0,y} + N_{xy} w_{0,xy} \\ & + N_{xy,y} w_{0,x} + N_{xy} w_{0,xy} - 2M_{xy,xy} + F = 0 \end{aligned} \tag{23}$$

Where

$$\sigma = D\varepsilon, N = A\varepsilon^0 + B\Upsilon, M = B\varepsilon^0 + C\Upsilon \tag{24}$$

$$\sigma = \begin{Bmatrix} \sigma_x \\ \sigma_y \\ \tau_{xy} \end{Bmatrix}, \quad N = \begin{Bmatrix} N_x - N_x^0 \\ N_y - N_y^0 \\ N_{xy} - N_{xy}^0 \end{Bmatrix}, \quad M = \begin{Bmatrix} M_x \\ M_y \\ M_{xy} \end{Bmatrix} \tag{25}$$

$$\begin{aligned} \{A_{ij}, B_{ij}, C_{ij}\} = & \int_{-\frac{h}{2}+h_p}^{-\frac{h}{2}} Q_{ij}^f \{1, z, z^2\} dz \\ & + \int_{-\frac{h}{2}}^{\frac{h}{2}} Q_{ij}^c \{1, z, z^2\} dz + \int_{\frac{h}{2}}^{\frac{h}{2}+h_p} Q_{ij}^f \{1, z, z^2\} dz \end{aligned} \tag{26}$$

Substituting Eqs. (25)-(26) into Eqs. (21)-(23) yields

$$\begin{aligned} & \frac{\partial^2 M_x}{\partial x^2} + 2\frac{\partial^2 M_{xy}}{\partial x \partial y} + \frac{\partial^2 M_y}{\partial y^2} \\ & = -\left( F + N_x \frac{\partial^2 w_0}{\partial x^2} + 2N_{xy} \frac{\partial^2 w_0}{\partial x \partial y} + N_y \frac{\partial^2 w_0}{\partial y^2} \right) \end{aligned} \tag{27}$$

Also, the compatibility equations in the case of large deformation are considered as (Asnafi and Abedi 2015)

$$\frac{\partial^2 \varepsilon_y^0}{\partial x^2} - \frac{\partial^2 \gamma_{xy}^0}{\partial x \partial y} + \frac{\partial^2 \varepsilon_x^0}{\partial y^2} = \left( \frac{\partial^2 w_0}{\partial x \partial y} \right)^2 - \frac{\partial^2 w_0}{\partial x^2} \frac{\partial^2 w_0}{\partial y^2} \tag{28}$$

In-plane forces can be expressed in terms of a stress function $\varphi(x, y)$, which is defined as (Chi and Chung 2006)

$$N_x = \frac{\partial^2 \varphi}{\partial y^2}, \quad N_y = \frac{\partial^2 \varphi}{\partial x^2}, \quad N_{xy} = -\frac{\partial^2 \varphi}{\partial x \partial y}, \tag{29}$$

The strains and the bending moment at the mid-surface are expressed in terms of the stress function $\varphi(x, y)$ and the deflection as follows

$$\varepsilon^0 = R\varphi + Y\Upsilon \tag{30}$$

$$M = -Y^T \varphi + J\Upsilon \tag{31}$$

$$\varphi = \begin{Bmatrix} \dfrac{\partial^2 \varphi}{\partial y^2} - N_x^0 \\ \dfrac{\partial^2 \varphi}{\partial x^2} - N_y^0 \\ \dfrac{\partial^2 \varphi}{\partial x \partial y} - N_{xy}^0 \end{Bmatrix} \tag{32}$$

$$R = A^{-1}, \quad Y = -A^{-1}B, \quad J = C - BA^{-1}B$$

By substituting Eq. (30) into Eq. (28), and Eq. (31) and Eq. (29) into Eq. (27) and also assume inertial and linear damping forces and then by using Galerkin technique, the nondimensional relation of w derived as follow

$$\ddot{W} + \lambda_1 \dot{W} + \lambda_2 W - \lambda_3 W^2 + \lambda_4 W^3 = \bar{F} \tag{33}$$

Where

$$\lambda_1 = \frac{c}{\alpha I_1}, \qquad \lambda_2 = 1 + \frac{\pi^2}{\alpha^2 I_1}\left( \frac{N_x}{a^2} + \frac{N_y}{b^2} \right),$$

$$\lambda_3 = \frac{16\pi^2 R_{12} h}{Y_{11} I_1 \alpha^2 a^2 b^2}, \quad \lambda_4 = \frac{\pi^4 h^2 (a^4 + b^4)}{16 Y_{11} I_1 \alpha^2 a^4 b^4},$$

$$\alpha^2 = \frac{\pi^4 (R_{12}^2 + Y_{11} J_{11})(a^2 + b^2)^2}{Y_{11} I_1 a^4 b^4}$$

$$\bar{F} = \frac{16}{\pi^2 \alpha^2 I_1 h} F, \qquad W = \frac{\bar{w}}{h}$$

In this section, the multiple scales perturbation method is used to solve the Eq. (33). Introducing the scale transformation parameter $\varepsilon$, the following equation can then be obtained

$$\ddot{W} + \varepsilon \lambda_1 \dot{W} + \omega_0^2 W - \varepsilon \lambda_3 W^2 + \varepsilon \lambda_4 W^3 = \varepsilon \bar{F} \tag{34}$$

Considering the case of parametric resonance of the system, the resonance relation can be represented as

$$\omega_0 = \omega + \varepsilon \sigma \tag{35}$$

where $\sigma$ is detuning parameter. The uniform solution for Eq. (34) can be expressed in the following form (Liu and Chu 2012)

$$w(t, \varepsilon) = w_0(T_0, T_1) + \varepsilon w_1(T_0, T_1) + \ldots \tag{36}$$

Where $T_0 = t$ and $T_1 = \varepsilon t$.

Substituting (36) and (35) into (34) and equating the coefficients of same power of $\varepsilon$ in the left and the right-hand sides of the equation, one can obtains the following differential equations:

Order $\varepsilon^0$

$$D_0^2 w_0 + \omega_0^2 w_0 = 0 \tag{37}$$

Order $\varepsilon^1$

$$\begin{aligned} D_0^2 w_1 + \omega_0^2 w_1 = & -2D_0 D_1 - \lambda_1 D w_0 + \lambda_3 w_0^2 \\ & -\lambda_4 w_0^3 + F \cos(\omega t) \end{aligned} \tag{38}$$

The solution for (37) in the complex form can be expressed as

$$w_0 = A_1(T_1)e^{i\omega_0 T_0} + \bar{A}_1(T_1)e^{-i\omega_0 T_0} \tag{39}$$

Substituting (39) into (38), yields

$$D_0^2 w_1 + \omega_0^2 w_1 = (-2i\omega_0 D_1 A_1 - i\omega_0\lambda_1 A_1 - 3\lambda_4 A_1^2\bar{A}_1 + \frac{F}{2}e^{i\sigma T_1})e^{i\omega_0 T_0} + CC + NST \tag{40}$$

where NST represents all non-secular terms and the symbol CC represents the complex conjugate terms. The secular terms should be zero, so that

$$2i\omega_0 D_1 A_1 + i\omega_0\lambda_1 A_1 + 3\lambda_4 A_1^2\bar{A}_1 - \frac{F}{2}e^{i\sigma T_1} = 0 \tag{41}$$

Where

$$A_1(T_1) = \frac{a(T_1)}{2}e^{i\beta(T_1)} \tag{42}$$

Substituting (42) into (41), and separating the real and imaginary parts in the resulting equations, the averaged equation can then be obtained as

$$D_1 a = -\lambda_1\frac{a}{2} + \frac{F}{2\omega_0}sin\,\phi \tag{43}$$

$$aD_1\phi = a\sigma - 3\lambda_4\frac{a^3}{8\omega_0} + \frac{F}{2\omega_0}cos\,\phi \tag{44}$$

Where $\phi = \sigma T_1 - \beta$.

The steady solutions of (43) and (44) correspond to steady motion of the system. In order to determine the amplitude and phase of steady solution, let $D_1 a = 0$, $D_1\phi = 0$. Therefore, one can obtain the algebraic equations of amplitude-frequency and phase-frequency as

$$c^2\frac{a^2}{4} + a^2\left(\omega - \omega_0 - 3\lambda_4\frac{\varepsilon a^2}{8\omega_0}\right)^2 = \left(\frac{F}{2\omega_0}\right)^2 \tag{45}$$

$$tan\,\phi = \frac{4\omega_0 c}{3\varepsilon\lambda_4 a^2 - 8\omega_0(\omega - \omega_0)} \tag{46}$$

## 3. Numerical results and discussions

In this section, different cases are examined due to nonlinear vibration and dynamic response of sandwich plate with considering FG core and CNTs reinforced nano-composite face sheets. The effects of various parameters are studied on the nonlinear frequency and dynamic response, such as temperature variation, thickness ratio (h/hp), volume fractions of carbon nanotubes, different property functions of FG core and power index of FG core.

The materials that are used in the bottom and top of core are SUS304 and Si3N4 that thermo mechanical properties listed in Table 1 by (Talha and Singh 2011).

The materials that are used in the matrix and resin of core are polymethylmethacrylate (*PMMA*) and single-walled carbon nanotubes (SWCNTs) (*tube length = 9.26 nm*, *tube mean radius = 0.68 nm*, *tube thickness = 0.067 nm*). The relationship between mechanical properties of matrix and resin with temperature change are expressed as (Mohammadimehr and Rostami 2018)

$$E_{11}^{CN}(T) = 6.1323\times10^{12} - 2.243\times10^{9}T + 2.08\times10^{6}T^2 \tag{47}$$

$$E_{22}^{CN}(T) = 7.6878\times10^{12} - 2.806\times10^{9}T + 2.6\times10^{6}T^2 \tag{48}$$

$$G_{12}^{CN}(T) = 1.6763\times10^{12} + 1.371\times10^{9}T - 1.59\times10^{6}T^2 \tag{49}$$

$$\alpha_{xx}^{CN}(T) = -4.434\times10^{-7} + 1.75765\times10^{-8}T - 1.5235\times10^{-11}T^2 \tag{50}$$

$$\alpha_{\theta\theta}^{CN}(T) = 5.4379\times10^{-6} - 9.905\times10^{-10}T + 3.05\times10^{-13}T^2 \tag{51}$$

$$E^m(T) = (3.52 - 0.0034T)\times10^9 \tag{52}$$

$$\alpha^m(T) = 45(1 + 0.0005\Delta T)\times10^{-6} \tag{53}$$

Table 2 presents the efficiency parameters of carbon nanotube for various volume fractions.

### 3.1 Validation of results

To validate the present studies, nonlinear frequency ratio

Table 1 Material properties of FG core

| | | $p_{-1}^T$ | $p_0^T$ | $p_1^T$ | $p_2^T$ | $p_3^T$ | $p(\text{at } 300k^0)$ |
|---|---|---|---|---|---|---|---|
| $Si_3N_4$ | E | $348.43\times10^9$ | $-3.07\times10^{-4}$ | $2.160\times10^{-7}$ | $-8.946\times10^{-11}$ | $322.2715\times10^9$ | $348.43\times10^9$ |
| | $\upsilon$ | 0.2400 | 0 | 0 | 0 | 0.2400 | 0.2400 |
| | $\alpha$ | $5.872\times10^{-6}$ | $9.095\times10^{-4}$ | 0 | 0 | $7.4746\times10^{-6}$ | $5.872\times10^{-6}$ |
| | $\rho$ | 2370 | 0 | 0 | 0 | 2370 | 2370 |
| SUS304 | E | $201.04\times10^9$ | $3.079\times10^{-4}$ | $-6.534\times10^{-7}$ | 0 | $207.7877\times10^9$ | $201.04\times10^9$ |
| | $\upsilon$ | 0.3262 | 2.002×10-4 | 3.397×10-7 | 0 | 0.3178 | 0.3262 |
| | $\alpha$ | 12.330×10-6 | 8.086×10-4 | 0 | 0 | 1.5321×10-5 | 12.330×10-6 |
| | $\rho$ | 8166 | 0 | 0 | 0 | 8166 | 8166 |

Table 2 The efficiency parameters of carbon nanotube for various volume fractions

| $V_{CNT}$ | $\eta_1$ | $\eta_2$ | $\eta_3$ |
|---|---|---|---|
| 0.12 | 0.137 | 1.022 | 0.715 |
| 0.17 | 0.142 | 1.626 | 1.138 |

Table 3 Nonlinear frequency ratios for simply supported square plates

| Method | $W_{max}/h$ | | | | |
|---|---|---|---|---|---|
| | 0.2 | 0.4 | 0.6 | 0.8 | 1 |
| Han and Petyt (1997) | 1.017 | 1.068 | 1.149 | 1.254 | 1.379 |
| Razavi and Shooshtari (2014) | 1.0168 | 1.065 | 1.142 | 1.2415 | 1.3586 |
| Present study | 1.015 | 1.083 | 1.157 | 1.253 | 1.381 |

for simply supported square isotropic plates ($a/h$ = 100, $\vartheta$ = 0.3) is obtained by present approach and are compared in Table 3 along with the previously published results.

### 3.2 Nonlinear vibration of sandwich plate

Fig. 2 presents time history of the dynamic responses [a) linear system b) nonlinear system] of the sandwich plate. In the case of a linear system, the behavior of the system will be regular and predictable but if the system is non-linear, the behavior of the system will be unplanned and unpredictable. Fig. 3 shows the effects of different property functions of FG core on response of the sandwich plate. In the case of ($n$ = 1), there is little difference between the responses of the system with the exponential and power index functions, but by increasing the ($n$), impressive difference is observed in the responses with exponential and power index functions.

The effects of nonlinearity on frequency responses of the steady state solution are analyzed that are shown in the Figs. 4-10. Fig. 4 represents the different property functions of FG core on amplitude–frequency diagram. At a constant nonlinear frequency, the amplitude of the system varies by changing the distribution of material in the sandwich plate core. Power index has maximum amplitude in nonlinear vibration of sandwich plate and sigmoid type has minimum ones. Fig. 5 presents the effect of power law index on amplitude–frequency diagram. Considering constant

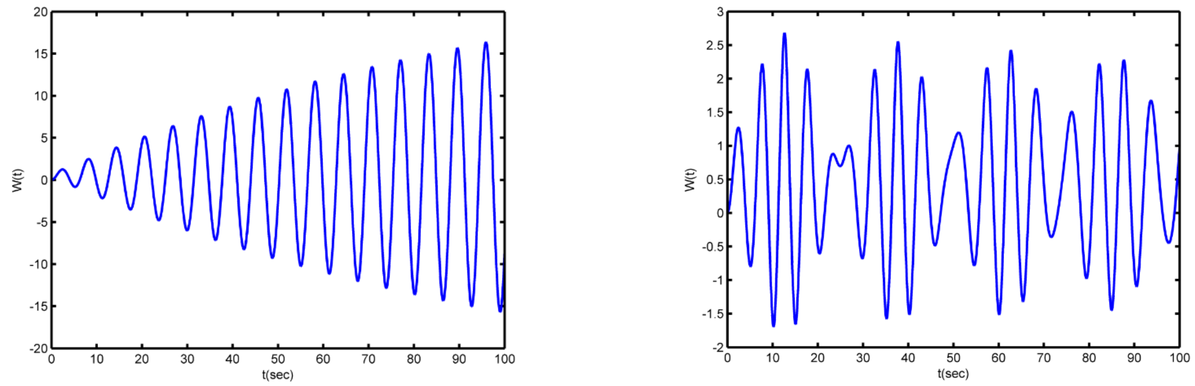


(a) Linear system (b) Nonlinear system

Fig. 2 Dynamic responses of sandwich plate ($a/b$ = 1, $a/h$ = 50, $h/h_p$ = 10, $T0$ = 300 k°, $\Delta T$ = 0, $V_{CNT}$ = 0.17, $n$ = 1, $c$ = 0, $F$ = 1, *power index type*)

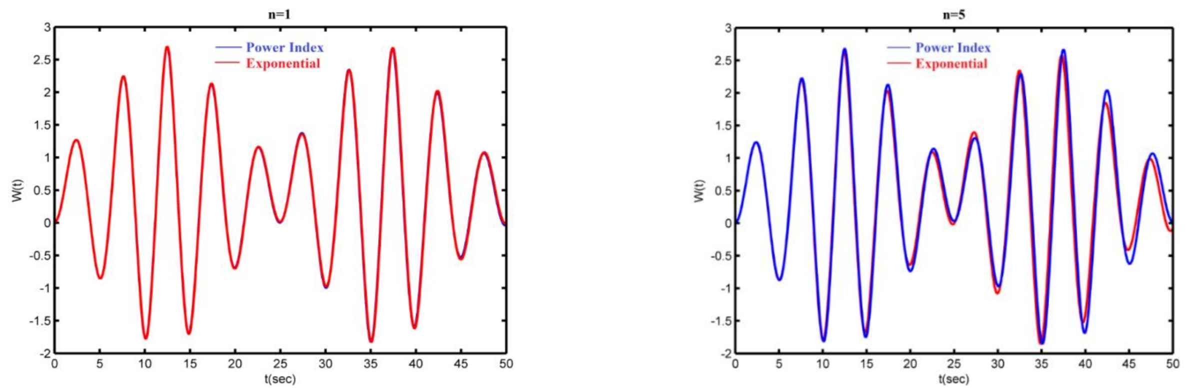


(a) $n$ = 1 (b) $n$ = 5

Fig. 3 The effect of property functions of FG core on time response of the sandwich plate ($a/b$ = 1, $a/h$ = 50, $h/h_p$ = 10, $T0$ = 300 k°, $\Delta T$ = 0, $V_{CNT}$ = 0.17, $c$ = 0, $F$ = 1)

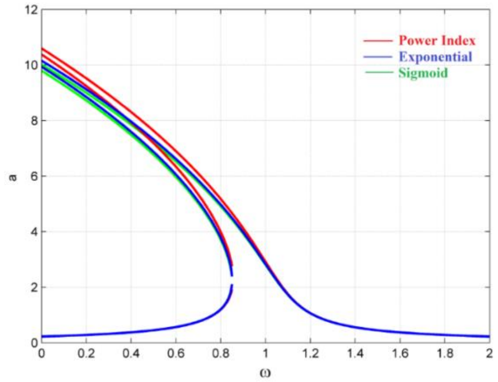


Fig. 4 The effect of property functions of FG core on amplitude–frequency response of the sandwich plate ($a/b = 1$, $a/h = 50$, $h/h_p = 10$, $T0 = 300$ k°, $\Delta T = 0$, $n = 5$, $V_{CNT} = 0.17$, $c = 0$, $\omega_0 = 1$, $e = -0.1$)

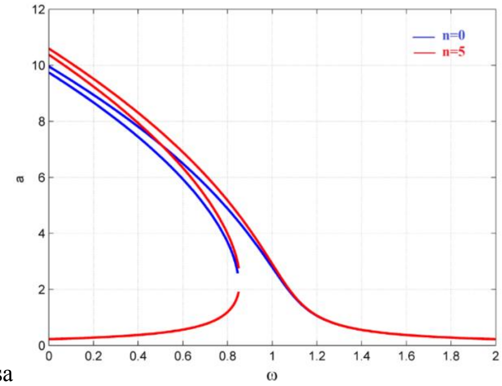


sa

Fig. 5 The effect power index of FG core on amplitude–frequency response of the sandwich plate ($a/b = 1$, $a/h = 50$, $h/h_p = 10$, $T0 = 300$ k°, $\Delta T = 0$, $V_{CNT} = 0.17$, $c = 0$, $\omega_0 = 1$, $e = -0.1$, *power index type*)

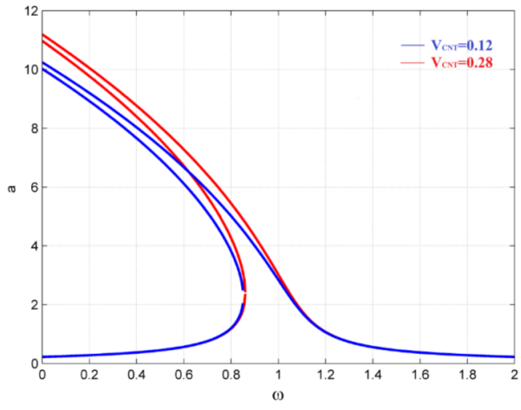


Fig. 6 The effect of volume fraction of carbon nanotube on amplitude–frequency response of the sandwich plate ($a/b = 1$, $a/h = 50$, $h/h_p = 10$, $T0 = 300$ k°, $\Delta T = 0$, $n = 5$, $c = 0$, $\omega_0 = 1$, $e = -0.1$, *power index type*)

nonlinear frequency, the more increment in the power law index the more the amplitude response of the system. The effect of volume fraction of carbon nanotube on nonlinear vibration of sandwich plate is showed in Fig. 6. By increasing volume fraction in constant frequency the amplitude of nonlinear frequency decreases. Fig. 7 investigates the effect of temperature variation on amplitude–frequency diagram. It can be seen that the temperature variation hasn't impressive effect on the

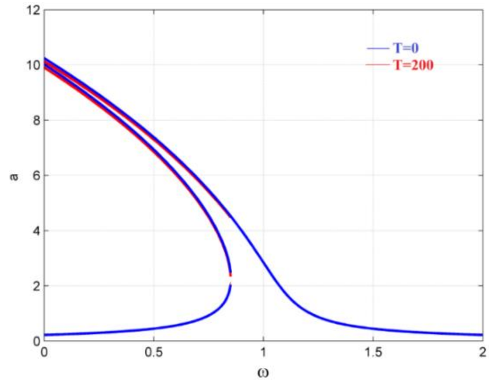


Fig. 7 The effect of temperature on amplitude–frequency response of the sandwich plate ($a/b = 1$, $a/h = 50$, $h/h_p = 10$, $T0 = 300$ k°, $V_{CNT} = 0.17$, $n = 5$, $c = 0$, $\omega_0 = 1$, $e = -0.1$, *power index type*)

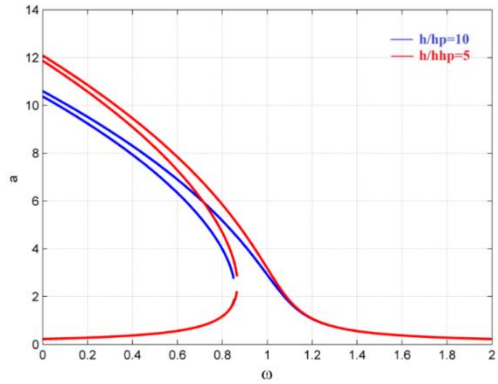


Fig. 8 The effect of thickness ratio on amplitude–frequency response of the sandwich plate ($a/b = 1$, $a/h = 50$, $T0 = 300$ k°, $\Delta T = 0$, $V_{CNT} = 0.17$, $n = 5$, $c = 0$, $\omega_0 = 1$, $e = -0.1$, *power index type*)

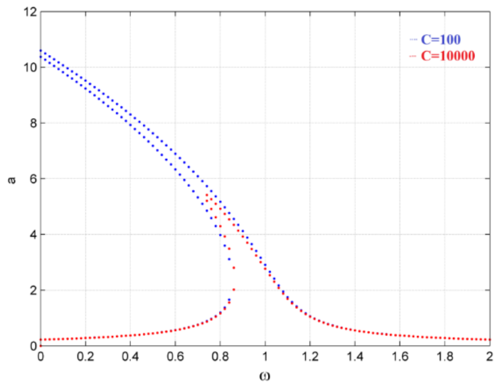


Fig. 9 The effect of linear damping factor on amplitude–frequency response of the sandwich plate ($a/b = 1$, $a/h = 50$, $h/h_p = 10$, $T0 = 300$ k°, $\Delta T = 0$, $V_{CNT} = 0.17$, $n = 5$, $\omega_0 = 1$, $e = -0.1$, *power index type*)

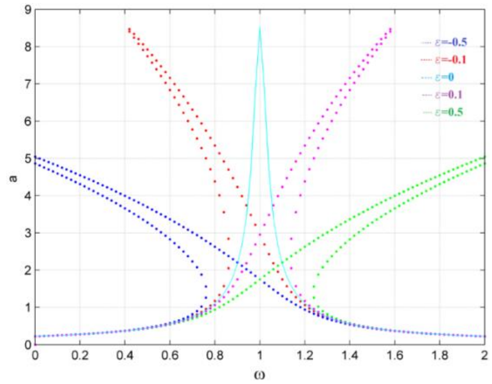


Fig. 10 The effect of scale transformation parameter on amplitude–frequency response of the sandwich plate ($a/b$ = 1, $a/h$ = 50, $h/h_p$ = 10, $T0$ = 300 k°, $\Delta T$ = 0, $V_{CNT}$ = 0.17, $c$ = 100, $n$ = 5, $\omega_0$ = 1, $e$ = -0.1, *power index type*)

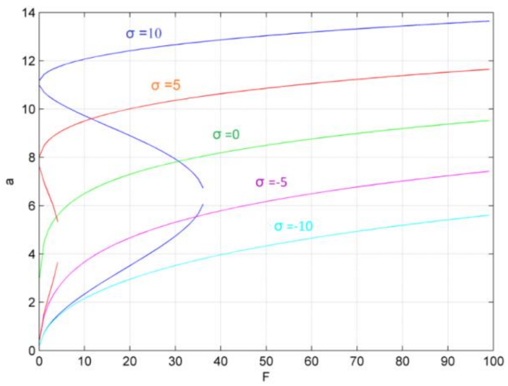


Fig. 11 Vibration amplitude under different frequency parameters

diagram. Fig. 8 illustrates the effects of face sheet and core thicknesses ratio ($h/h_p$) on amplitude–frequency diagram. The effect of linear damping factor on amplitude–frequency response is showed in Fig. 9. It can be seen that by increasing the linear damping factor of sandwich plate, the amplitude decreases. According to Fig. 10, in the case of $\varepsilon < 0$, the system stiffness presents softening behavior, while in the case of $\varepsilon > 0$, the system stiffness becomes hardening. The system is linear when $\varepsilon = 0$, where the system stiffness keeps neither softening behavior nor hardening behaviour. Fig. 11 shows the relationship between the response amplitude and excitation amplitude. If $\sigma = -5$, $\sigma = -10$ or $\sigma = 0$, the response amplitude is only corresponding to the excitation. In the cases of $\sigma = 5$ or $\sigma = 10$ a unique excitation can be correspond many solutions of the response amplitude (bifurcation).

## 4. Conclusions

In this paper, we studied the nonlinear vibration of sandwich plate with considering functionally graded material core and nanocomposite layers. Classical plate theory was used for modeling the behavior of sandwich plate. The governing equations of motion were derived by using Hamilton's principle and then, by using the Galerkin technique and multiple scales perturbation method were solved and the relation between amplitude and nonlinear frequency was found. This study focuses on the frequency responses and dynamic responses of system. It is tried to analysis the effects of the excitation, power law index of FG core, volume fraction of carbon nanotube, property function of FG core, variation of temperature, scale transformation parameter and linear damping factor on frequency responses of steady state solution and nonlinear amplitude - frequency diagram.

The results indicate that:

- The behavior of the linear system will be regular and predictable but if the system is non-linear, the behavior of the system will be unplanned and unpredictable.
- By increasing the (n), impressive difference appears in the system response for the exponential and power index functions.
- Increasing the volume fraction of carbon nano-tube, the stiffness of the system increases, so in a constant deflection of sandwich plate, with increasing the volume fraction, the nonlinear frequency of the system also increases.
- The changes in the temperature within the allowable range for nanocomposite material behavior has little effect on the nonlinear frequency of the system.
- Owing to the factor of nonlinearity, the system stiffness has become hardening or softening, in other words, appears hard spring characteristic or soft spring characteristic.

## Acknowledgments

The research described in this paper was financially supported by the Natural Science Foundation.

## References

Alijani, F. and Amabili, M. (2013), "Nonlinear vibrations of laminated and sandwich rectangular plates with free edges. Part 1: Theory and numerical simulations", *Compos. Struct.*, **105**, 422-436. https://doi.org/10.1016/j.compstruct.2013.05.034

Asnafi, A. and Abedi, M.A. (2015), "A complete analogical study on the dynamic stability analysis of isotropic functionally graded plates subjected to lateral stochastic loads", *Acta Mech.*, **226**(7), 2347-2363. https://doi.org/10.1007/s00707-015-1321-7

Chaudhari, V.K., Gupta, A. and Talha, M. (2016), "Nonlinear Vibration response of shear deformable functionally graded plate using finite element method", *Proceedings of the 3rd International Conference on Innovations in Automation and Mechatronics Engineering*. https://doi.org/10.1016/j.protcy.2016.03.018

Chi, S.H. and Chung, Y.L. (2006), "Mechanical behavior of functionally graded material plates under transverse load—Part I: analysis", *Int. J. Solids Struct.*, **43**, 3657-3674. https://doi.org/10.1016/j.compstruct.2013.05.034

Chien, R.D. and Chen, C.S. (2005), "Nonlinear vibration of laminated plates on a nonlinear elastic foundation", *Compos. Struct.*, **70**, 90-99.

https://doi.org/10.1016/j.compstruct.2004.08.015
Chien, R.D. and Chen, C.S. (2006), "Nonlinear vibration of laminated plates on an elastic foundation", *Thin-Wall. Struct.*, **44**, 852-860. https://doi.org/10.1016/j.tws.2006.08.016
Darabi, M. and Ganesan, R. (2017), "Nonlinear dynamic instability analysis of laminated composite thin plates subjected to periodic in-plane loads", *Nonlinear Dyn.*, **91**, 187-215. https://doi.org/10.1007/s11071-017-3863-9
Duc, N.D., Cong, P.H. and Quang, V.D. (2016), "Nonlinear dynamic and vibration analysis of piezoelectric eccentrically stiffened FGM plates in thermal environment", *Int. J. Mech. Sci.*, **115**, 711-722. https://doi.org/10.1007/s11071-017-3863-9
Fan, Y., Xiang, Y., Shen, H.S. and Hui, D. (2018), "Nonlinear low-velocity impact response of FG-GRC laminated plates resting on viscoelastic foundations", *Compos. Part B: Eng.*, **144**, 184-194. https://doi.org/10.1016/j.compositesb.2018.02.016
Gholamia, R. and Ansari R. (2018), "Nonlinear harmonically excited vibration of third-order shear deformable functionally graded graphene platelet-reinforced composite rectangular plates", *Eng. Struct.*, **156**, 197-209. https://doi.org/10.1016/j.engstruct.2017.11.019
Han, W. and Petyt, M. (1997), "Geometrically nonlinear vibration analysis of thin, rectangular plates using the hierarchical finite element method—I: The fundamental mode of isotropic plates", *Comput. Struct.*, **63**(2), 295-308. https://doi.org/10.1016/S0045-7949(96)00345-8
Houmat, A. (2013), "Nonlinear free vibration of laminated composite rectangular plates with curvilinear fibers", *Compos. Struct.*, **106**, 211-224. https://doi.org/10.1016/j.compstruct.2013.05.058
Kattimani, S.C. and Ray, M.C. (2014), "Smart damping of geometrically nonlinear vibrations of magneto-electro-elastic plates", *Compos. Struct.*, **114**, 51-63. https://doi.org/10.1016/j.compstruct.2014.03.050
Liu, Y. and Chu, F. (2012), "Nonlinear vibrations of rotating thin circular cylindrical shell", *Nonlinear Dyn.*, **67**, 1467-1479. https://doi.org/10.1007/s11071-011-0082-7
Mohammadimehr, M. and Rostami, R. (2018), "Bending and vibration analyses of a rotating sandwich cylindrical shell considering nanocomposite core and piezoelectric layers subjected to thermal and magnetic fields", *Appl. Mathe. Mech.*, **39**(2), 219-240. https://doi.org/10.1007/s10483-018-2301-6
Mohammadimehr, M., Rostami R. and Arefi, M. (2016a), "Electro-elastic analysis of a sandwich thick plate considering FG core and composite piezoelectric layers on Pasternak foundation using TSDT", *Steel Compos. Struct., Int. J.*, **20**(3), 513-544. https://doi.org/10.12989/scs.2016.20.3.513
Mohammadimehr, M., Rousta Navia, B. and Ghorbanpour Arani, A. (2016b), "Modified strain gradient Reddy rectangular plate model for biaxial buckling and bending analysis of double-coupled piezoelectric polymeric nanocomposite reinforced by FG-SWNT", *Compos. Struct. part B: Eng.*, **87**, 132-148. https://doi.org/10.1016/j.compositesb.2015.10.007
Nematollahi, M.S. and Mohammadi, H. (2019), "Geometrically nonlinear vibration analysis of sandwich nanoplates based on higher-order nonlocal strain gradient theory", *Int. J. Mech. Sci.*, **156**, 31-45. https://doi.org/10.1016/j.ijmecsci.2019.03.022
Razavi, S. and Shooshtari, A. (2014), "Nonlinear free vibration of magneto-electro-elastic rectangular plates", *Compos. Struct.*, **119**, 377-384. https://doi.org/10.1016/j.compstruct.2014.08.034
Shahverdi, H. and Khalafi, V. (2016), "Bifurcation analysis of FG curved panels under simultaneous aerodynamic and thermal loads in hypersonic flow", *Compos. Struct.*, **146**, 84-94. https://doi.org/10.1016/j.compstruct.2016.03.011
Shen, H.S. and Xiang, Y. (2014), "Nonlinear vibration of nanotube-reinforced composite cylindrical panels resting on elastic foundations in thermal environments", *Compos. Struct.*, **111**, 291-300. https://doi.org/10.1016/j.compstruct.2014.01.010
Singha, M.K. and Daripa, R. (2009), "Nonlinear vibration and dynamic stability analysis of composite plates", *J. Sound Vib.*, **328**, 541-554. https://doi.org/10.1016/j.jsv.2009.08.020
Solanki, M.K., Mishra, S.K., Shukla, K.K. and Singh, J. (2015), "Nonlinear free vibration of laminated composite and sandwich plates using multiquadric collocations", *Proceedings of the 4th International Conference on Materials Processing and Characterization*. https://doi.org/10.1016/j.matpr.2015.07.210
Soni, S., Jain, N.K. and Joshi, P.V. (2017), "Analytical modeling for nonlinear vibration analysis of partially cracked thin magneto-electro-elastic plate coupled with fluid", *Nonlinear Dyn.*, **90**,137-170. https://doi.org/10.1007/s11071-017-3652-5
Talha, M. and Singh, B.N. (2011), "Thermo-mechanical induced vibration characteristics of shear deformable functionally graded ceramic—metal plates using finite element method", *Proceedings of the Institution of Mechanical Engineers, Part C: Journal of Mechanical Engineering Science*, **225**(1), 50-65. https://doi.org/10.1243/09544062JMES2115
Teng, M.W. and Wang, Y.Q. (2020), "Nonlinear free vibration of rectangular plates reinforced with 3D graphene foam: Approximate analytical solution", *Results in Physics*, **17**. https://doi.org/10.1016/j.rinp.2020.103147.
Torabi, J. and Ansari, R. (2017), "Nonlinear free vibration analysis of thermally induced FG-CNTRC annular plates: Asymmetric versus axisymmetric study", *Comput. Methods Appl. Mech. Eng.*, **324**, 327-347. https://doi.org/10.1016/j.cma.2017.05.025
Xue, C.X., Pan, E., Han, Q.K., Zhang, S.Y. and Chu, H.J. (2011), "Non-linear principal resonance of an orthotropic and magnetoelastic rectangular plate", *Int. J. Non-Linear Mech.*, **46**, 703-710. https://doi.org/10.1016/j.ijnonlinmec.2011.02.002
Yang, J., Huang, X.H. and Shen, S.H. (2020), "Nonlinear vibration of temperature-dependent FG-CNTRC laminated plates with negative Poisson's ratio", *Thin Wall. Struct.*, **148**. https://doi.org/10.1016/j.tws.2019.106514
Zeng, S. Wang, B.L. and Wang, K.F. (2019), "Nonlinear vibration of piezoelectric sandwich nanoplates with functionally graded porous core with consideration of flexoelectric effect", *Compos. Struct.*, **207**, 340-351. https://doi.org/10.1016/j.compstruct.2018.09.040

*CC*